# PERSISTENT PHOSPHORS FOR PAINTING, MEDICAL AND BIOLOGICAL APPLICATIONS

**M. Nazarov**

*Institute of Applied Physics, Academiei str. 5, Chisinau, MD-2028 Republic of Moldova*

(Received 30 April 2013)

## Abstract

Multiphase micro and nanoparticle persistent phosphors are synthesized and applied for different fields including painting, medical and biological investigations. A lot of examples show a broad range of applications of persistent luminescence from bulk materials to high tech products, especially in medicine. The development of high efficiency nanosized phosphor makes it possible to propose persistent materials as very good candidates for photodynamic therapy of cancer. An artificial block from slag, concrete, and sand covered with $SrAl_2O_4:Eu^{2+}$, $Dy^{3+}$ based phosphor is prepared, and a new direction in biology for algae cultivation and artificial reef is discussed. For the first time, underwater luminescence is experimentally studied under real sea conditions. Bright blue-green long-lasting afterglow is registered at a depth of 5 m. The fishes are attracted by the light of the artificial reef.

## 1. Introduction

Persistent phosphors are a type of phosphors that have very long persistent afterglow emission. The phenomenon of afterglow is as follows. After the excitation source is turned off, emission from previously trapped electrons is still observed. The irradiation used may be UV, visible light, X-ray, gamma radiation as well as usual sun light.

The mechanism of long persistent phosphors' phosphorescence is basically a three-level electron transition mechanism, including a ground state, an excited state, and a meta-stable trapping state. Phosphorescence lifetime is usually longer than the lifetime at the excited state, and it depends on the trap depth and trapping/detrapping mechanism.

Persistent luminescence has been intriguing to people for hundreds of years. The situation drastically changed about 17 years ago when Matsuzawa et al. discovered bright and long-lasting luminescence in $SrAl_2O_4:Eu^{2+},Dy^{3+}$ [1]. In 1996, they reported a new type of long persistent phosphor $SrAl_2O_4:Eu^{2+},Dy^{3+}$ with a strong emission at 520 nm (green), which is developed from a phosphor $SrAl_2O_4:Eu^{2+}$ found by Abbruscato in 1971 [2]. Takasaki et al. reported similar results [3]. They found an afterglow with both a far higher initial intensity and a much longer lifetime compared to traditional ZnS:Cu,Co. The persistence time of $SrAl_2O_4:Eu^{2+},Dy^{3+}$ was extended to longer than 16 h (reported persistent time varied with detection limits from 10 to 20 h) after codoping with $Dy^{3+}$.

A short time later, a similar long persistent phosphor $CaAl_2O_4:Eu^{2+}$, $Nd^{3+}$ was reported with a blue emission at 450 nm [4]. These two phosphors drew considerable attention from many scientists because a 16-h persistent time could bring phosphorescence over a whole night [5-8]. Since then, long persistent phosphor becomes one of the major research areas in luminescence materials.

Recent long persistent phosphors researches are focused on two directions. The first direction is in fundamental research on the physics of trapping/detrapping mechanism. It eventually is associated with the energy level structure of emission centers in the host band gap [9], and the excited state dynamics of the optical electrons [10]. In this direction, researches on alkali earth aluminates doped with $Ce^{3+}$ generated some important conclusions that trapping/detrapping mechanisms were closely related to electron delocalization and relocalization processes [11, 12]. After a series of thermoluminescence [11], photoconductivity [12], and thermal conductivity measurements [13], electron delocalization was found to be associated with electron-phonon interaction at a dopant-host overlapped energy level [14].

The other direction is the development of new long persistent phosphors, in which red long persistent phosphors were of particular interest. Many new long persistent phosphors have been found within this decade, such as alkali earth aluminates doped with $Ce^{3+}$, $Mn^{2+}$, $Tb^{3+}$ [13, 15, 16], alkali earth silicates doped with $Mn^{2+}$, or $Eu^{2+}/Dy^{3+}$ [16-18], alkali earth oxide doped with $Eu^{3+}$ [19], rare earth oxides and oxysulfides doped with $Er^{3+}$, $Eu^{3+}$, $Ti^{4+}$ and $Mg^{2+}$ [20-23], and some other individual systems such as Zn phosphate doped with $Mn^{2+}$ etc [24, 25].

Some novel methods have been developed while people are developing new long persistent phosphor systems. These methods include co-doping with ions as electron traps, co-doping ions to create defects for defect related electron traps, persistent energy transfer, etc.

These investigations have led to a renewed research interest, and it promoted the use of these persistent phosphors in signalization, traffic signs, power switch, traffic police uniforms, luminous paints, glow-in-the-dark toys, decorative objects, emergency signage, watches and clocks, dials and displays, textile printing, medical diagnostics, and many other applications.

Applications of persistent luminescence phosphors are rapidly expanding from bulk materials visible to everyone (e.g., exit signalization on airplane cabin floors) to high tech products. In this study, we consider traditional applications, such as painting, and more interesting and important applications in medicine and biology. We propose also a new direction in study and application these materials, namely underwater investigations of persistent luminescence for an artificial reef and algae cultivation. A new multiphase blue-green persistent phosphor based on $SrAl_2O_4$ was synthesized and applied under real sea conditions. The synthesis of persistent luminescence micro and nanoparticles with appropriate optical properties and the chemical modification of their surface are reported in this study.

## 2. Experimental

The examined materials for different applications were prepared by two methods: solid state reaction and combustion synthesis. The conventional solid state reaction is mostly used for the preparation of bulk phosphors used in traditional applications as safety signs, watch dials, decorative objects, and toys. The combustion method is used for preparing nanoparticle materials which we need in medicine and sometimes in biology.

### 2.1. Solid state reaction

Strontium aluminate phosphor doped with $Eu^{2+}$ and co-doped with $Dy^{3+}$ ($SrAl_2O_4:Eu^{2+}$, $Dy^{3+}$) for traditional applications were prepared by solid state reaction approach using strontium carbonate ($SrCO_3$; Aldrich, 99.9 %), aluminum oxide ($Al_2O_3$), europium oxide ($Eu_2O_3$; Aldrich, 99.99 %) and dysprosium oxide ($Dy_2O_3$; Aldrich, 99.99 %) as the starting materials. Small amount (0.2 mol %) of $H_3BO_3$ was used as a flux. Prior to heating at 1250ºC, the reagents were ground using a ball mill to form a homogeneous mixture. First, the dry milling was used for 30

min and then continued by wet-mixing machine for 30 min. The resulting slurry was dried at 150°C for 3 h to remove the water content. After fully dried, the mixed white powder was placed in a small alumina crucible and then fired at 1250°C for 2 h under a mild reducing atmosphere. Graphite crucible was used to create the reducing atmosphere and to ensure complete reduction of $Eu^{3+}$ to $Eu^{2+}$ and to crystallize and form the luminescence centers. Usually the particle size in this process is about 10-20 μm. The mixing–milling process was used after calcination to prepare smaller particle size and homogenous mixture.

### 2.2. Combustion synthesis

Similar nanoparticles of $SrAl_2O_4:Eu^{2+}$ phosphor were prepared by combustion synthesis. The starting material included: Aluminium nitrate ($Al(NO_3)_3.9H_2O$; Systerm, 98%), strontium nitrate ($Sr(NO_3)_2$; Aldrich, 99%), europium oxide ($Eu_2O_3$; Aldrich, 99.99%) and urea ($CO(NH_2)_2$; Systerm, 99%). Small amounts of acid boric ($H_3BO_3$; Fisher, 100.04%) were used as a flux and small amounts of urea were used as a reducer and fuel. Figure 1 shows the flow chart of $SrAl_2O_4:Eu^{2+}$ powders synthesis.

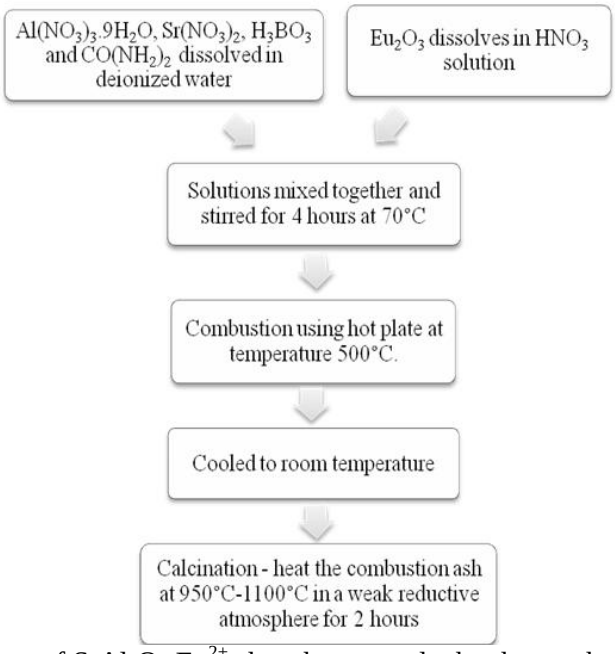


**Fig. 1.** Flow chart of $SrAl_2O_4:Eu^{2+}$ phosphors powder by the combustion synthesis.

There are some details below to describe the combustion synthesis.

The stoichiometric quantities of raw materials were calculated and weighed using a high precision mass balance. The composition of the acid boric was set as 0.08 mol %. Each of the raw materials $Al(NO_3)_3.9H_2O$, $Sr(NO_3)_2$, $H_3BO_3$ and $CO(NH_2)_2$ was dissolved into 20 ml of deionized water, respectively, to obtain a transparent solution. Wet mixing was used to obtain a homogeneous mixture. Deionized water is selected instead of distilled water due to the removal of the mineral ions, such as cations from sodium, calcium, iron, copper and anions from chloride and bromide, which will influence the experiment result [26]. $Eu_2O_3$ was dissolved with a minimum amount of a $HNO_3$ solution to convert into $Eu(NO_3)_3$ according to equation (1):

$$Eu_2O_3 + 6HNO_3 \rightarrow 2\ Eu(NO_3)_3 + 3H_2O \quad (1)$$

The two solutions were mixed together and stirred using a magnetic bar for several hours at 75°C to obtain a viscous gel solution. The mixing temperature is set in the range between 70 and 80°C in this project for several reasons. Firstly, according to the MSDS, aluminum nitrate has a fairly low melting point (73°C) but a high boiling point or decomposition temperature (135°C). The heating of aluminum nitrate above its melting point leads to the formation of a homogeneous solution. Furthermore, it is possible to dissolve acid nitric, which has a low boiling point (83°C).

The resulting mixed viscous gel continues for combustion reaction. In this project, combustion is done by using a hot plate instead of using a furnace. White combustion ash was obtained in 3-5 min by combusting the precursor gel at a temperature of 500°C. Initially, the solution boiled and underwent dehydration followed by decomposition with emission of large amounts of gasses (oxides of carbon, nitrogen, and ammonia). Later, the viscous gels spontaneously start to burn and burn slowly without flame (smouldering combustion), thus producing a white fined powder. The whole process takes less than 5 min. When heated at 500°C, the powder was hold for a few minutes to ensure the combustion reaction was complete. The chemical equation of combustion is complicated and not yet verified; however, the brief equation can be shown as below:

$$2Al(NO_3)_3.9H_2O + Sr(NO_3)_2 + CO(NH_2)_2 + Eu(NO_3)_3 + 1.5O_2 \rightarrow SrAl_2O_4 : Eu^{2+} + 20H_2O + 5N_2 + 14.5O_2 + CO_2 \quad (2)$$

Next, the combustion ash was cooled to room temperature.

The final pigment synthesis is done by heating the combustion ash at 950−1100°C in a weak reductive atmosphere for 2 h to obtain $SrAl_2O_4:Eu^{2+}$ phosphor. The weak reductive atmosphere was created by using a graphite crucible to inhibit further oxidation.

Other compositions of persistent phosphors were synthesized by similar methods.

## 3. Results and discussion

### 3.1. Persistent materials in paints and plastics

The combination of long persistence with relative environmental stability has led to the fact that these materials are used as pigments in paints and plastics for safety and security applications. For example, many of the stairwells and exits in buildings, as well as airplane cabin floors, have persistent phosphor markings to guide inhabitants out of the building/airplane in emergency situations. It is also likely that if you have a glow-in-the-dark paint or part that glows blue or green in the dark, these phosphor powders are incorporated into those paints or parts. These applications for luminescent and display materials were completely enabled by the discovery of the $MAl_2O_4:Eu^{2+}$, $RE^{3+}$ ( M= Sr, Ca etc) family of phosphors. The moisture sensitivity of $(Ca,Sr)Al_2O_4$ hosts has led to two separate fields of study: the development of protective coatings for persistent phosphor powders and the invention and development of blue and green persistent phosphors that are not as sensitive to moisture and environmental conditions. There is also interest in developing red persistent phosphors to enable a full palette of persistent phosphor colors when combined with the blue and green luminescence of $CaAl_2O_4:Eu^{2+},RE^{3+}$ and $SrAl_2O_4:Eu^{2+},RE^{3+}$, respectively. The idea of mutating a well established and commercially available phosphor for other luminescence applications, such as $Y_2O_2S:Eu^{3+}$, though reinforced with co-dopants, such as $Mg^{2+}$ and $Ti^{IV}$, does not always result in a superior persistent luminescence material, as was the case with $SrAl_2O_4:Eu^{2+}$. The design of new efficient persistent

luminescence phosphors requires more than this, or a lot of luck. While red persistent phosphors in nitride hosts have been improved [27], the duration and intensity of persistence is still not comparable to that of aluminate phosphors. But, in any case, the full palette of colors of persistent materials was made (Figs. 2– 4).

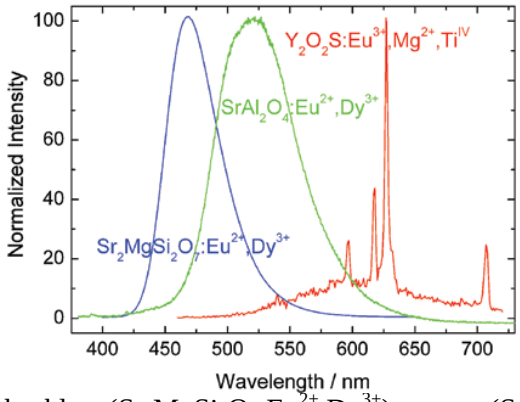


**Fig. 2.** Luminescence spectra of the blue ($Sr_2MgSi_2O_7:Eu^{2+},Dy^{3+}$), green ($SrAl_2O_4:Eu^{2+},Dy^{3+}$), and red ($Y_2O_2S:Eu^{3+}$ ,$Mg^{2+}$, $Ti^{IV}$) emitting phosphors after UV excitation [28] .


**Fig. 3.** Blue, red, pink, violet, yellow, and green colors are possible in glow dark paint.

**Fig. 4.** Phosphorescent paint.

Phosphorescent paint is commonly called "glow-in-the-dark" paint. It is made from different phosphors, such as silver-activated zinc sulfide, or, more recently, doped strontium aluminate, and typically glows a pale green to greenish blue color. The mechanism for producing light is similar to that of fluorescent paint, but the emission of visible light persists for some time after it has been exposed to light. Phosphorescent paints have a sustained glow which lasts for up to 12 h after exposure to light, but will eventually fade over time.

This type of paint has been used to mark escape paths in aircraft and for decorative use, such as "stars" applied to walls and ceilings (Fig. 5).


**Fig. 5.** Glow-in-the-Dark Rocket, Planets and Stars Wall Stick.

Some other examples of glow-in-the-dark application are shown in Figs. 6-9.

**Fig. 6.** Hand-painted glow-in-the-dark blue Angelfish art magnet.

**Fig.7.** Luminescent paint by Pieter van den Bosch.

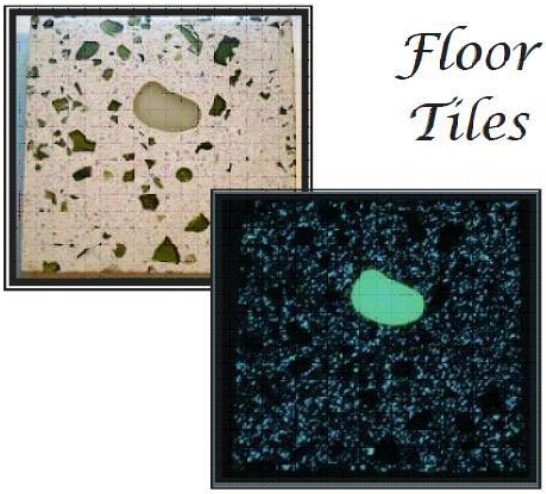


**Fig. 8.** Decorative floor tiles.

**Fig. 9.** A helmet and a high-voltage insulator (ceramic) in the day time and at dark.

### 3.2 Medical application

With the development of high efficiency nanosized red phosphor, it has become possible to incorporate it in organic matrices to produce singlet oxygen, which kill cancer cells (Fig. 10). This persistent phosphor is a very good candidate for photodynamic therapy (PDT) of cancer. Other light sources include light-emitting diodes (LEDs), which may be used for surface tumors, such as skin cancer [29]. Researchers continue to study ways to improve the effectiveness of PDT and expand its use to other cancers.

Over 2 mln people annually lost due to cancer. Photodynamic therapy has near 100% efficiency. PDT combines a drug (called a photosensitizer or photosensitizing agent) with a specific type of light to kill cancer cells. When photosensitizers are exposed to a specific wavelength of light, they produce a form of oxygen that kills nearby cells [30-36] (Fig. 10). PDT may also be repeated and may be used with other therapies, such as surgery, radiation, or chemotherapy [32, 33].

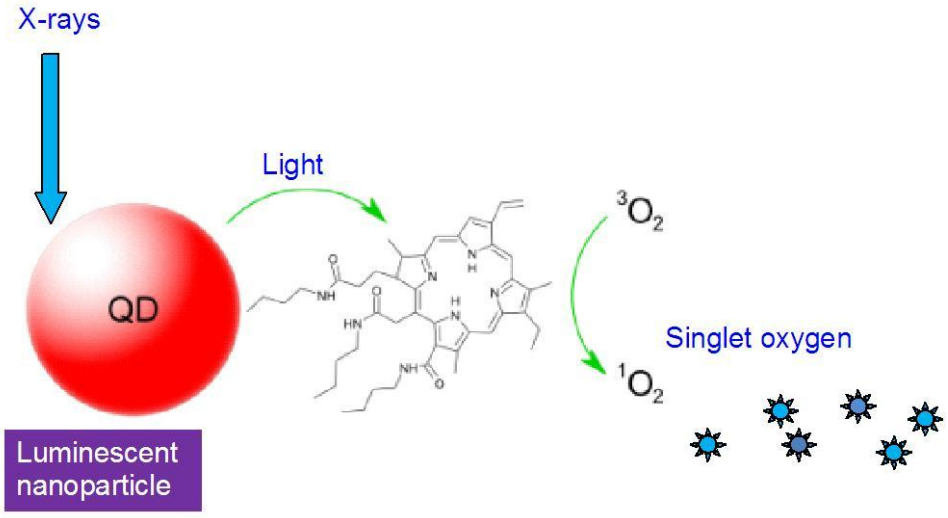


**Fig. 10.** Cancer therapy using luminescent nanoparticles, which produces red light and then singlet oxygen when irradiated with X-rays.

Each photosensitizer is activated by light of a specific wavelength [34-38]. This wavelength determines how far the light can travel into the body [29, 34-36]. Thus, doctors use specific photosensitizers and wavelengths of light to treat different areas of the body with PDT.

In the first step of PDT for cancer treatment, a photosensitizing agent is injected into the bloodstream. The agent is absorbed by cells all over the body but stays in cancer cells longer than it does in normal cells. Approximately 24 to 72 h after injection [30, 31], when most of the agent has left normal cells but remains in cancer cells, the tumor is exposed to light. The photosensitizer in the tumor absorbs the light and produces an active form of oxygen that destroys nearby cancer cells [30-36].

The light used for PDT in traditional application can come from a laser or other sources [29, 32, 33] (Fig. 11).

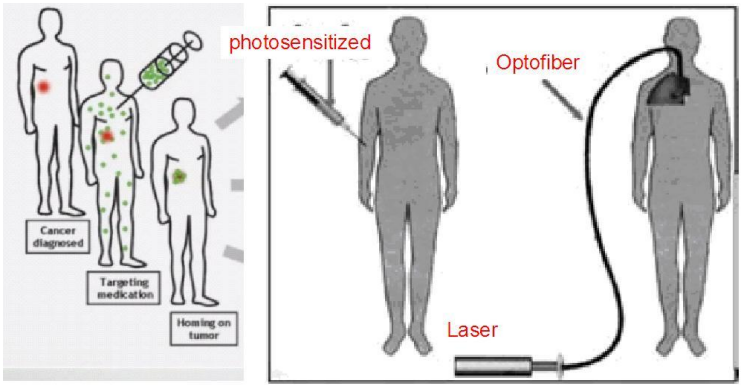


**Fig. 11.** Laser light is directed through fiber optic cables.

Laser light can be directed through fiber optic cables (thin fibers that transmit light) to deliver light to areas inside the body [32, 33]. For example, a fiber optic cable can be inserted through an endoscope (a thin, lighted tube used to look at tissues inside the body) into the lungs or esophagus to treat cancer in these organs, but it is difficult in application for internal organs. Therefore, the cancer therapy using luminescent nanoparticles instead of optic cables seems to be promising and more efficient. One of the aims of our work is to use a red persistent nontoxic nanosized phosphor exposed to X-ray inside the body as a new photosensitizer and produce a form of oxygen that kills nearby cancer cells

Some examples of synthesized nanophosphors with red emission are shown in Fig. 12.

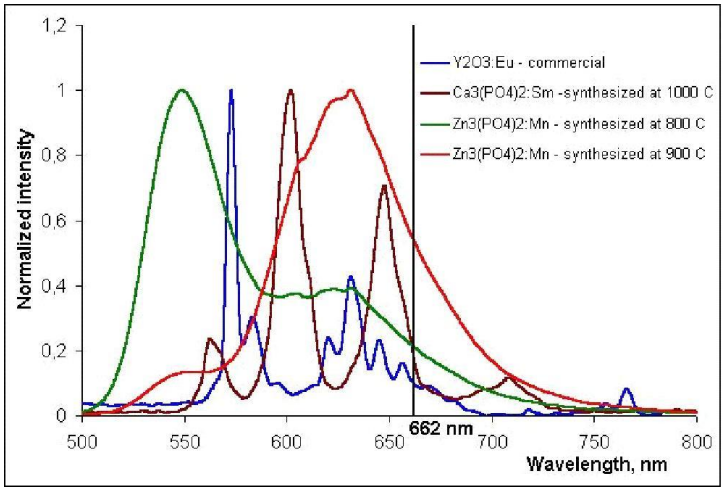


**Fig. 12.** Red phosphors for medical application: ZnS:Cu, ZnS:Cl ($\lambda_{max}$=450-550 nm), $Zn_3(PO_4)_2$:Mn ($\lambda_{max}$ = 630 nm), $Ca_3(PO_4)_2$:Sm ($\lambda_{max}$ = 648 nm), $Y_2O_3$:Eu ($\lambda_{max}$ = 612 nm).

The elaboration of persistent luminescence mechanisms is advancing at a rapid pace, and these problems have been basically solved, though the refinement of the details is still needed. In terms of application, the challenge of finding an efficient red emitting persistent phosphor is still waiting.

### 3.3. Biological application

There is a risk of forever damaging the existence of thousands natural reefs because of tsunami or other cataclastic phenomena. We need to know how to restore or sometimes to improve reefs and marine ecosystems. Therefore, measuring and interpreting the impact of human actions on the diversity on marine and oceanic life represent one way to prevent ecological disasters and predict possible environmental changes.

An artificial rock and block made of steel slag hybrid matrix have been recently developed in Japan [39, 40]. Electric Arc Furnace (EAF) slag is a byproduct from steelmaking process with an estimated amount generated of about 10-15 wt % for every ton of steel produced [41]. Steel slag is used in the production of cement [41], coastal marine blocks for seaweed bed [42], and substrate for mangrove rehabilitation [43]. Steel slag has also been shown to be effective in corral growing due to a significant amount of calcium and silicon present in its composition [44]. Steel slag can be modified to form potassium calcium silicate ($K_2CaSiO_4$) [42]. This mineral has been of interest in the field of applied mineralogy due to the crystal structure which slowly dissolves in acidic soils providing valuable nutrients [45]. Its production from steelmaking slag is a renewable resource and allows for greater waste recycling from steelmaking process. It can also be found in products, such as the ashes from biomass combustion [46]. The production of this fertilizer is from iron slag after the desiliconization process of hot metal in the steel mill [42, 47]. The main mineral phase present was $K_2Ca_2Si_2O_7$ [48]. However, researchers are yet to clarify the actual chemical composition of the mineral phase present in this compound and the mechanism of its dissolution as a fertilizer [46].

We propose an experimental artificial glow reef made from steel slag and from concrete and sand to provide a hard surface. Another decision is to cover this artificial reef as well as real corals by persistent phosphors. The main goal of these experiments is to cultivate the algae in the future and to attract the fishes. An artificial block from concrete and sand covered with $SrAl_2O_4:Eu^{2+}$, $Dy^{3+}$ based phosphor was prepared, and a new direction in study and application of persistent phosphors was proposed. For the first time, underwater luminescence was experimentally studied under real sea conditions. Our pioneers works in this field have been recently published [49, 50].

In this present study, the Scheil-Gulliver model was applied to slag solidification to characterize the solidification behavior of mineral phase formation in a modified EAF slag system. Details of the solidification modeling have been described elsewhere [51]. In the experimental work, EAF slag from a Malaysian steel company was modified with 20 wt % $K_2CO_3$. Each powder mixture was placed in an alumina crucible and melted in a Lenton EHF 1700 furnace. Details of the experimental work have been described elsewhere [52]. The plant chosen for the study was Typhonium flagelliforme or better known in Malay as “Keladi Tikus”. Typhonium flagelliforme is a medicinal herb plant that belongs to the Araceae family [53]. For the plant fertilization study, three conditions were investigated. These conditions were in a Deionized water (DI) without fertilizer, DI with Potassium Silicate Slag (PSS) fertilizer and DI with PSS coated by an epoxy layer with persistent $SrAl_2O_4:(Eu^{2+},Dy^{3+})$ phosphors. The phosphors coating was prepared to investigate the effect of fertilizer absorption due to enhanced photosynthesis activity. Persistent phosphors can emit light for a long time from seconds to many hours after the excitation has ended. The irradiation used may be UV, visible light, X-ray, gamma radiation, as well as usual sun light.

The results of solidification model for slag system are given in Fig. 13. For 0.6 $CaO/SiO_2$ wt ratio, after complete solidification, six mineral phases were formed, with their percentage fraction given in Fig. 13. Potassium silicates (PS) started to form at 650$^oC$ and reached a

maximum composition of 27.5 wt % at 605°C where the solidification ends. Detailed analysis of effect of $CaO/SiO_2$ wt ratio with respect to PS formed is given elsewhere [54].

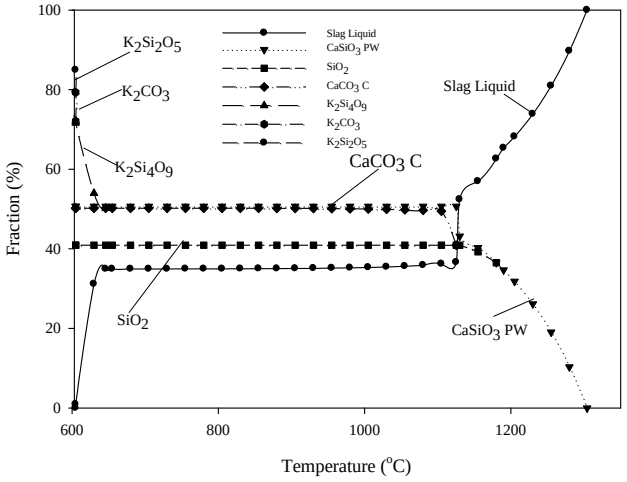


**Fig. 13.** Fractions of a simulated mineral phase during solidification at 1330–600°C ($CaO/SiO_2$= 0.6).

The mineralogical compositions of the modified PSS samples were analyzed by XRD and shown in Fig. 14. The diffraction patterns of the slags showed that there are heterogeneous materials consisting of mixtures of crystalline and amorphous phases. According to Fig. 14, three crystalline phases were identified in the air cooled synthetic slag (EAF0A): potassium silicate ($K_2Si_2O_5$), silicon dioxide ($SiO_2$) and alpha calcium silicate (□-$CaSiO_3$). In the water cooled synthetic slag (EAF0W), three crystalline phases were detected: alpha calcium silicate (□-$CaSiO_3$), potassiu $_{25}$).

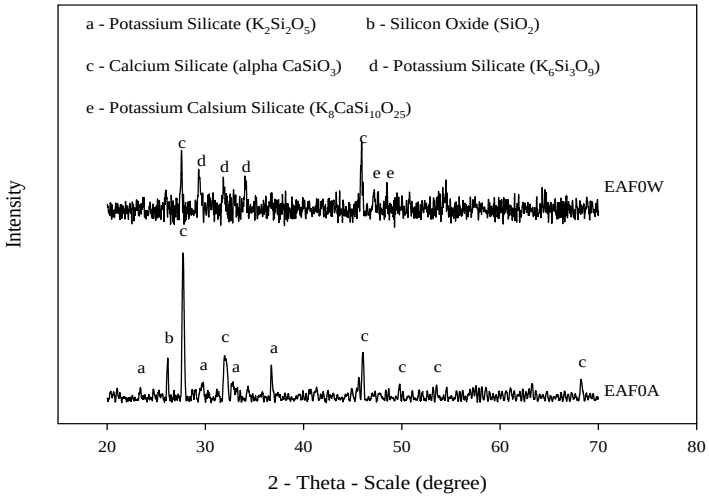


**Fig. 14.** XRD pattern of modified synthetic EAF slags system. EAF0A =Air cooled with 0.6 wt. ratio of $CaO/SiO_2$ and EAF0W =Water cooled with 0.6 wt. ratio of $CaO/SiO_2$.

Initial plant fertilization by PSS was studied on Typhonium flagelliforme in DI water under different conditions. Figure 15 shows the pH relationship to different fertilization conditions. It is evident from Fig. 15 that the pH values increased within the first 24 h in all the plants before slowly settling to an optimum condition after 400 h. The plants grown with DI only settled at a pH of 5 which is close to pH produced by 2 wt % of citric acid. The acidic nature of the Typhonium flagelliforme is well suited to the application of PSS [55]. This is due to the neutralization that will occur with the basic PSS. On the other hand, the plants with PSS and coated PSS fertilization settled at a basic pH. Both conditions showed a similar trend in the pH values variation with time, settling at around 8.9 and 8.7. However, the coated PSS had a slightly lower pH value. This can be attributed to the phosphor coatings which slowed the release of nutrients from the PSS fertilizer. The content of nitrogen, potassium, calcium, silicon, and phosphorus of the leaves with respect to the fertilization conditions will be studied in the future. It has been shown that a higher potassium and silicon uptake by plants is expected with PSS fertilization [56]. This in turn will lead to a better plant growth and disease immunity [57].

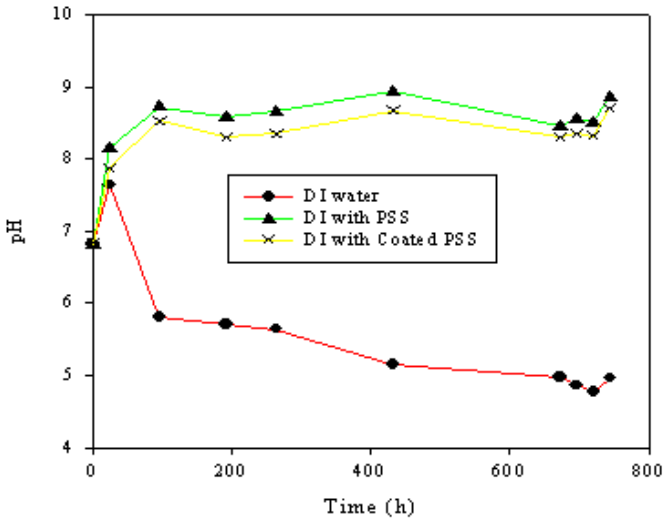


**Fig. 15.** pH measurement of Typhonium flagelliforme under different fertilization conditions.

Below we show some applications of artificial reefs from metallic construction and slag with persistent phosphors under real sea conditions near the Malaysia in the Indian Ocean.

**Fig. 16.** Real coral on a metallic construction (Pulau Kapas).

**Fig. 17.** Artificial coral reefs (Pulau Kapas).

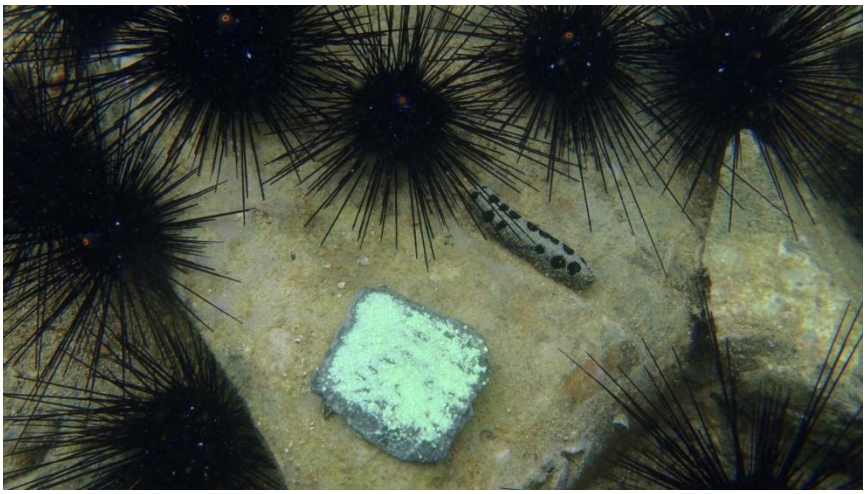

**Fig. 18.** Green luminescence from slag covered with persistent $SrAl_2O_4:Eu^{2+},Dy^{3+}$ surrounded by sea-urchins.

**Fig. 19**. Artificial luminescent block inside real corals.

**Fig. 20.** Real coral with phosphor inside.

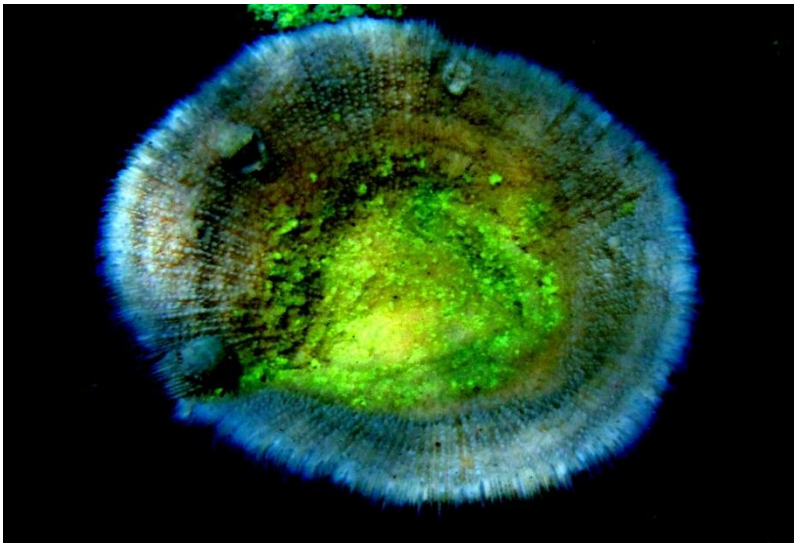

**Fig. 21.** Night luminescence of real coral covered with phosphor.

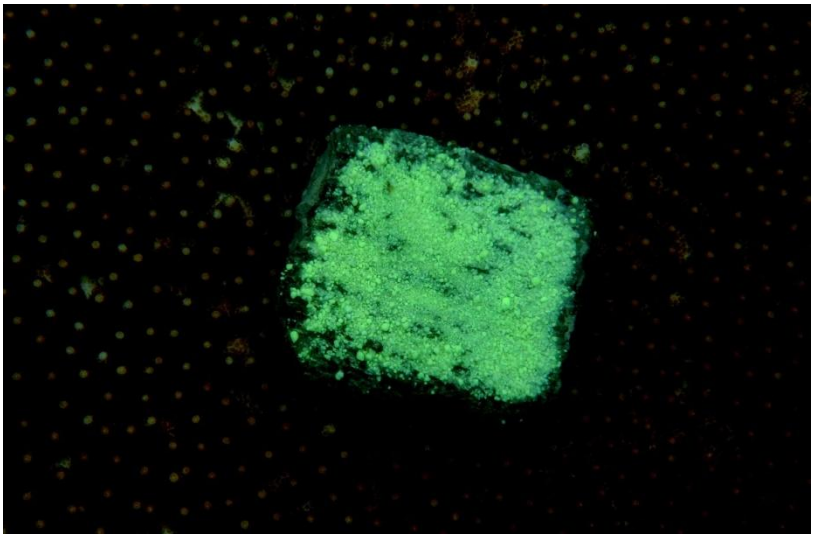

**Fig. 22.** Night luminescence of artificial slag covered with phosphor.

**Fig. 23.** The clown fishes are attracted by the bright light of an artificial reef.

## 4. Conclusions

Multiphase micro and nanoparticle blue-green persistent phosphor with turquoise luminescence was synthesized and applied for painting, medical and biological investigations.

A lot of examples show a very large range of applications of persistent luminescence phosphors from bulk materials visible to everyone to high tech products, especially in medicine. The development of high efficiency nanosized phosphor gives the possibility to incorporate it in an organic matrix to produce singlet oxygen, which kill cancer cells. This persistent phosphors are very good candidates for photodynamic therapy of cancer.

For the first time, the experiments with an artificial stone covered with $SrAl_2O_4:Eu^{2+}$, $Dy^{3+}$ based phosphor were carried out under real sea conditions in Pulay Payar Marine Park Malaysia. Strong, and bright blue-green (turquoise) luminescence was observed and registered under water. The fishes were attracted by the light of the artificial reef. The model of a slag system for the subsequent algae cultivation is proposed.

## References

[1] T. Matsuzawa, Y. Aoki, N. Takeuchi, and Y. Murayama, J. Electrochem. Soc 143, 2670 (1996).
[2] V. Abbruscato, J. Electrochem. Soc. 118, 930 (1971).
[3] H. Takasaki, S. Tanabe, and T. Hanada, J. Ceram. Soc. Jpn 104, 322 (1996).
[4] H. Yamamoto and T. Matsuzawa, J. Lumin. 72, 287 (1997).
[5] E. Nakazawa and T. Mochida, J. Lumin. 72-74, 236 (1997).
[6] T. Katsumata, T. Nabae, K. Sasajima, S. Komuro, and T. Morikawa, J. Electrochem Soc. L 243 (1997).
[7] T. Katsumata, R. Sakai, S. Komuro, T. Morikawa, and H. Kimura., J. Crys. Grow. 198/199, 869 (1999).
[8] W. Jia, H. Yuan, L. Lu, H. Liu, and W. M. Yen, J. Lumin. 76-77, 424 (1998).
[9] C. W. Thiel, H. Cruguel, Y. Sun, G. J. Laypeyre, R. M. Macfarlane, R. W. Equall, and R. L. Cone, J. Lumin. 94-95, 1 (2001).

[10] D. Jia, R. S. Meltzer, and W. M. Yen, J. Lumin. 99, 1 (2002).
[11] D. Jia and W. M. Yen, J. Electrochem. Soc. 150, H61 (2003).
[12] D. Jia, X. Wang, W. Jia, and W. M. Yen, J. Lumin. (2005)
[13] D. Jia, X. Wang, and W. M. Yen, Chem. Phys. Lett. 363-364, 241 (2002).
[14] D. Jia, J. Lumin. 117, 170 (2006).
[15] D. Jia, X. Wang, E. v. d. Kolk, and W. M. Yen, Opt. Comm. 204, 247 (2002).
[16] X. Wang, D. Jia, and W. M. Yen, J. Lumin 102-103, 34 (2003).
[17] Q. Fei, C. Chang, and D. Mao, J. Alloy. Comp. 390, 133 (2005).
[18] G. B. Zhang, Z. M. Qi, H. J. Zhou, Y. B. Fu, T. L. Huo, X. X. Luo, and C. S. Shi, J. El. Spec. Rel. Phen. 144–147, 861 (2005).
[19] J. Fu, Electrochem. Solid Stat. Lett 3, 350 (2000).
[20] P. Zhang, Z. Hong, M. Wang, X. Fang, G. Qian, and Z. Wang, J. Lumin. 113, 89 (2005).
[21] X. Wang, Z. Zhang, Z. Tang, and Y. Lin, Mater. Chem. Phys. 80, 1 (2003).
[22] Y. Lin, C. Nan, N. Cai, X. Zhou, H. Wang, and D. Chem, J. Alloy. Comp. 361, 92 (2003).
[23] B. Lei, Y. Liu, G. Tang, Z. Ye, and C. Shi, Mater. Chem. Phys. 87, 227 (2004).
[24] J. Wang, S. Wang, and Q. Su, J. Solid Stat. Chem. 177, 895 (2004).
[25] J. Wang, Q. Su, and S. Wang, Mat. Res. Bul. 40, 590 (2005).
[26] J. J. Moore and H. J. Feng, Prog. Mater Sci. 39, 243 (1995).
[27] Y. Miyamoto, H. Kato, Y. Honna, H. Yamamoto, and K. Ohmi, J. Electrochem. Soc. 156, J235 (2009).
[28] J. Holsa, Electrochem. Soc. Interface 43 (2009).
[29] E. Skovsen, J. Snyder, J. Lambert, and P.Ogilby, J. Physi. Chem. B 109, 8570 (2005).
[30] S. Wang, J Chen, L Keltner, J Christophersen, F Zheng, M Krouse, and A. Singhal, Cancer Journal 8, 154 (2002).
[31] N. Lane, New Light on Medicine, Scientific American, 2003.
[32] M. Hamblin and T. Hasan, Photochem. Photobiol. Sci. 3, 436 (2004).
[33] L. Huang, T Dai, and M. Hamblin, Methods Mol Biol. Methods in Molecular Biology 635, 155 (2010).
[34] R. Boumedine and D. Roy, Cytotherapy 7, 134 (2005).
[35] C. Mulroney, S. Gluck, and A. Ho, Semin Oncol 21, 24. (1994)
[36] M. Ochsner, Arzneimittelforschung 47, 1185 (1997).
[37] H. Tang, M. Hamblin, and C. Yow, J. Infect. Chemother. 13, 87 (2007).
[38] T. Maisch, S Hackbarth, J. Regensburger, A. Felgentrager, W. Baumler, M. Landthaler, and B. Roder, J. Dtsch. Dermatol. Ges. 9, 360 (2011).
[39] T. Takahashi and K. Yabuta, NKK Tech. Rev. 87 (2002).
[40] N. Isoo, J. Jpn. Soc. Fisheries Sci. 66, 647 (2000).
[41] A. S. Reddy, R. K. Pradhan, and S. Chandra, Int. J. Mineral Proc. 79, 98 (2006).
[42] T. Takahashi and K. Yabuta, NKK Tech. Rev. 87, 38 (2002).
[43] S. Day, W. J. Streever, and J. J. Watts, Restoration Ecology 7, 139 (1999).
[44] T. A. Mohammed, H. Aa, H. Nf, E. E.-A. Ma, and E.-M. Khm, Int. J. Environm. Protect. 2, 5 (2012).
[45] T. Akiyama, Y. Yasuko, and M. Seiichi, Jpn. J. Soil Sci. Plant Nutrition 72, 484 (2001).
[46] E. Arroyabe, R. Tessadri, D. M. To¨bbens, and V. Kahlenberg, J. Am. Ceram. Soc. 94, 2652 (2011).
[47] NKK, 2000.
[48] T. Akiyama, Y. Yao, and S. Matsuno, Jpn. J. Soil Sci. Plant Nutrition 72, 484 (2001).

[49] M. Nazarov, A. Nor Nazida, M.N Ahmad-Fauzi, and P. Ivannikov, Microscopy Analysis 27 (2013).
[50] M. Nazarov, A. Nor Nazida, M.N Ahmad-Fauzi, A.Badri Ismail, and P. Ivannikov, Mold. J. Phys. Sci. 11, 147 (2012).
[51] L. K. Bankole, S. A. Rezan, and N. M. Sharif, SEAISI Quarterly Journal 40, 26 (2011).
[52] L. K. Bankole, S. A. Rezan, and N. M. Sharif, Adv. Mater. Res. 620, 66 (2012).
[53] D. A. A. Bardi, M. A. S. Khan, S. Z. Sabri, F. A. Kadir, A. A. Mahmood, A. A. Zahra, S. M. Suzy, N. Al-Hanhana, and A. Al-Magrami, Sci. Res. Essays 6, 3232 (2011).
[54] L. K. Bankole, S. A. Rezan, and N. M. Sharif, SEAISI Quarterly Journal 40, 7 (2011).
[55] Y. Tokunaga, Fertilizer Research 30, 55 (1991).
[56] UC SAREP, (University of California Sustainable Agriculture Research and Education Program for USDA National Organic Program USA, ed.), 2003.
[57] T. A. Branca and V. Colla, in Material Recycling - Trends and Perspectives (D. Achilias, ed.), InTech, Italy, 2012, p. 406.